ACS MATERIALS LETTERS

www.acsmaterialsletters.org

LETTER

Stable, Bromine-Free, Tetragonal Perovskites with 1.7 eV Bandgaps via A-Site Cation Substitution

Ziru Huang, Bin Chen, Laxmi Kishore Sagar, Yi Hou, Andrew Proppe, Hao-Ting Kung, Fanglong Yuan, Andrew Johnston, Makhsud I. Saidaminov, Eui Hyuk Jung, Zheng-Hong Lu, Shana O. Kelley, and Edward H. Sargent*

Cite This: *ACS Materials Lett.* 2020, 2, 869–872

Read Online

ACCESS | Metrics & More | Article Recommendations | Supporting Information

ABSTRACT: Metal halide perovskite absorbers with wide bandgaps (1.6–1.7 eV) that are suitable for tandem devices typically require high Br concentrations; this renders the material prone to halide segregation and degradation. Inorganic, bromine-free CsPbI3 has a wide bandgap of 1.7 eV and does not suffer from halide segregation; however, these active layers are not stable at room temperature. Here, we report a method to create stable tetragonal perovskites with a bandgap near 1.7 eV: we add small amounts of large A-site cations having ionic radii between 272 and 278 pm—dimethylammonium (DMA) and guanidinium (Gua)—into the crystal lattice. When we deploy perovskites using mixed Cs and these large organic cations, we achieve stable, wide bandgap perovskites with power conversion efficiencies of 15.2% and V_{OC} of 1.19 V. This study extends materials selection for wide bandgap Cs-based perovskites.

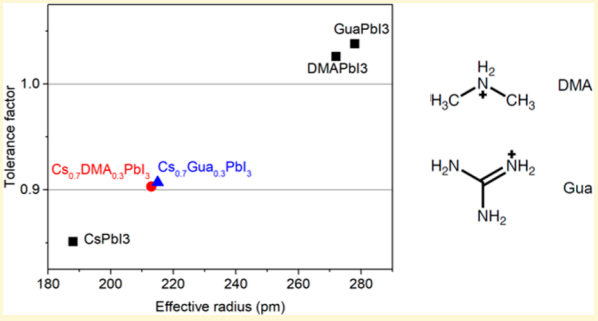

Metal halide perovskites have attracted attention because of their application in low-cost, high-efficiency photovoltaics.[1] To make tandem solar cells with Si, a perovskite bandgap of 1.7 eV is optimal,[2] but usually requires compositions that contain 30–40% bromine (such as $MAPbI_{0.6}Br_{0.4}$ and $CsFAMAI_{0.6}Br_{0.4}$).[3−5] These compositions undergo I–Br phase segregation, lowering device stability and efficiency.[6]

To overcome halide segregation, it is desirable to minimize the Br concentration, but this lowers the bandgap to values that are suboptimal for tandem solar cells. Fully inorganic perovskites that use only iodine in their composition, such as $CsPbI_3$, can achieve wide bandgaps, but are not phase stable.[7] For stable CsFA and CsMA mixtures, the ratio of Cs cannot exceed 30%, and the resulting compositions exhibit smaller bandgaps.[8] Because of the small radius of the Cs^+ ion, larger cations are needed to stabilize perovskite structures with Cs concentrations exceeding 30%. To maintain both a wide bandgap and phase stability in bromine-free perovskites, a lower concentration of larger organic cations is needed.

Here, we report bromine-free perovskites with bandgaps near 1.7 eV. We demonstrate that, by using A-site cations with ionic radii between 272 and 278 pm—DMA and Gua—we are able to create perovskites that are phase-stable at room temperature. Compared to conventional cubic CsMAFA perovskites, we find the $Cs_{1-x}DMA_xPbI_3$ and $Cs_{1-x}Gua_xPbI_3$ perovskites exhibit tetragonal structures—a finding which we ascribe to the presence of the larger cation in the crystal lattice. In photovoltaic devices, we achieved a PCE of 15.2% using $Cs_{1-x}DMA_xPbI_3$, comparable to the PCE achieved in 40% Br wide bandgap perovskites. The operational stability of the $Cs_{1-x}DMA_xPbI_3$ devices is 230 h, nearly 20 times longer than that of 40% Br wide bandgap perovskites.

The phase instability of α-$CsPbI_3$ arises due to the small ionic radius of Cs^+ cation, which results in a tolerance factor lower than that required for a stable perovskite phase.[9,10] $CsPbI_3$ undergoes a phase transition to the non-perovskite δ-phase due to this instability, also accelerated by lattice distortions induced by polar solvents.[7,11,12] Figure 1 and Table 1 show the tolerance factors of $CsPbI_3$, $DMAPbI_3$,

Received: April 24, 2020
Accepted: June 16, 2020
Published: June 16, 2020

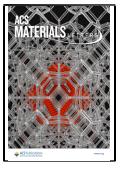

https://dx.doi.org/10.1021/acsmaterialslett.0c00166
ACS Materials Lett. 2020, 2, 869–872

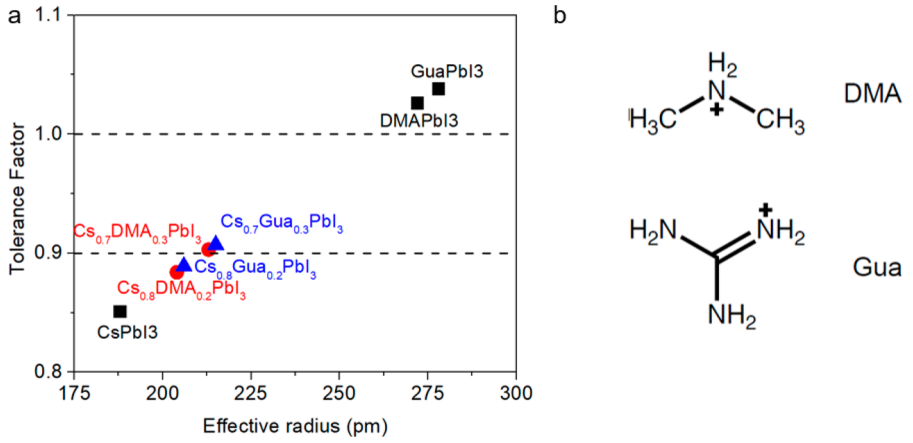

Figure 1. Tuning tolerance factor using mixed CsDMA and CsGua. (a) Tolerance factors of pure $CsPbI_3$, pure $DMAPbI_3$, pure $GuaPbI_3$, $Cs_{1-x}DMA_xPbI_3$ and $Cs_{1-x}Gua_xPbI_3$. (b) Molecular structure of DMA and Gua.

Table 1. Comparison of Ionic Radii for Different A-Site Cations

cation	ionic radius (pm)	tolerance factor for pure $APbI_3$
DMA	272	1.026
Gua	278	1.038
MA	217	0.911
Cs	181	0.851

$GuaPbI_3$, and mixed CsDMA and CsGua perovskites. For pure CsPbI3, the cubic phase gives a tolerance factor of 0.851, which is not in the range of structurally stable perovskites. Pure DMA and Gua cations are too large and give tolerance factors greater than 1; but mixed CsDMA and CsGua compositions reach a tolerance factor slightly above 0.9 ($Cs_{0.7}DMA_{0.3}PbI_3$ gives 0.903 and $Cs_{0.7}Gua_{0.3}PbI_3$ gives 0.907), which falls within the favorable range for a stable perovskite phase.

We first examined the crystallinity and morphology of thin films of CsDMA and CsGua perovskites. Figure 2 a, b gives the morphology of the films under scanning electron microscope (SEM). The films exhibit smooth surfaces that are free of pinholes. Figure 2 c, d show X-ray diffraction (XRD) patterns of CsDMA and CsGua films. In a previous report, CsDMA perovskites synthesized at 100°C were assumed to be cubic,[9] but the double peaks at 28° in that report suggested that the structure may actually be tetragonal. In this work, we anneal the film between 40 to 80°C, and the resulting XRD shows a tetragonal structure. Compared to normal tetragonal

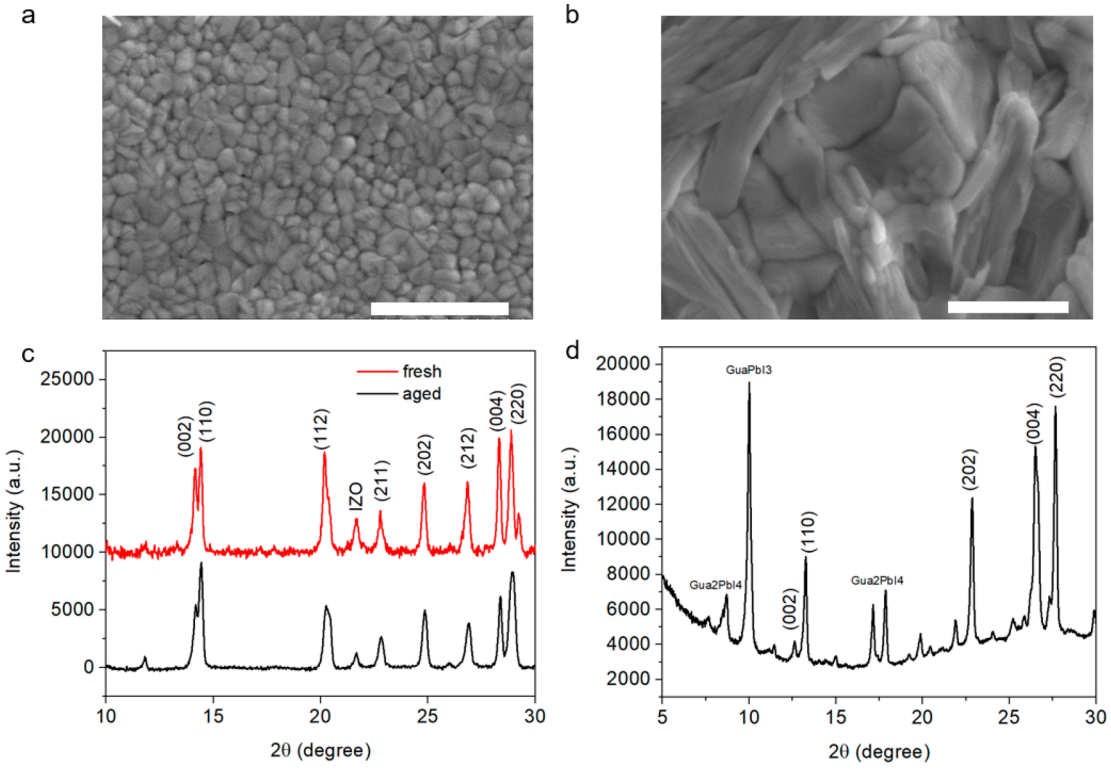

Figure 2. Morphology and crystallization of CsDMA and CsGua perovskite. (a) SEM images for CsDMA and (b) CsGua perovskite. The scale bar is 1 μm. (c) XRD pattern of fresh and aged CsDMAperovskite film and (d) XRD pattern of CsGua perovskite.

https://dx.doi.org/10.1021/acsmaterialslett.0c00166
ACS Materials Lett. 2020, 2, 869−872

$CsPbI_3$(β-CsPbI3), pure β-CsPbI3 is only observed above 210 °C, but for CsDMA and CsGua, the perovskite phase is formed between room temperature and 80 °C. This mixture method extends the range for stable, Cs-based perovskite. To confirm the presence of DMA/Gua in the annealed films, we carried out X-ray photoelectron spectroscopy (XPS) measurements (Figure S1). The N signal indicates that the large organic cations are present in the film following annealing at 80 °C.

Next, we monitored the stability of perovskite by obtaining XRD before and after ageing. Figure 2c gives a comparison of XRD patterns for the CsDMA perovskite. After samples age in air for 30 min, the XRD pattern of the CsDMA perovskite remains the same (Figure 2c), while in the case of pure $CsPbI_3$, it degrades considerably (Figure S2). We performed thermal gravimetric analysis (TGA) to asses thermal stability, and found no mass change below 200 °C (Figure S3), indicating that the CsDMA films are more thermally stable than perovskite compositions containing volatile MA molecules.[13]

After witnessing the ambient stability of the perovskite system, we proceeded to examine its optoelectronic properties. We collected steady state photoluminescence (PL) spectra and PL lifetimes of the CsDMA and CsGua perovskite films (Figure 3). The $Cs_{0.7}DMA_{0.3}$ perovskite exhibits a PL emission

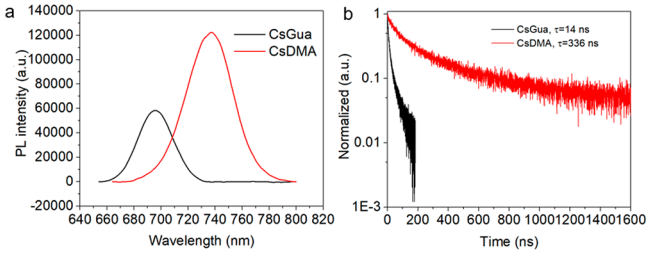

Figure 3. Photoluminescence spectroscopy of CsDMA and CsGua thin films: (a) Steady-state PL spectra and (b) PL lifetime of CsGua and CsDMA perovskite.

peak at 730 nm, corresponding to a bandgap at 1.70 eV, and the $Cs_{0.7}Gua_{0.3}$ perovskite gives a PL emission peak at 690 nm, corresponding to a bandgap at 1.79 eV. This bandgap is similar to that of pure $CsPbI_3$ and is well-chosen for front cells in perovskite-Si (1.70 eV) and perovskite-perovskite tandems (1.79 eV). The PL lifetime of $Cs_{0.7}DMA_{0.3}$ and $Cs_{0.7}Gua_{0.3}$ perovskite are 336 ns and 14 ns. Compared to pure CsPbI3, which gives a PL lifetime between 1 to 5 ns depending on the fabrication process,[14,15] the mixed tetragonal perovskite gives a substantially longer PL lifetime comparable to the normal CsFA perovskite,[16] suggesting reduced nonradiative recombination. We conclude that the mixed perovskite has a lower trap state density—a finding that should allow for a higher V_{oc} in perovskite solar cells (PSC). Pure $CsPbI_3$ PSCs usually suffer from a large V_{oc} loss: the highest reported V_{oc} is only 1.11 V, despite $CsPbI_3$ exhibiting a wide bandgap at 1.70 eV.

We, therefore, proceeded to investigate the effects of mixed tetragonal CsDMA and CsGua perovskites on the performance of solar cells. We fabricated planar PSCs with an architecture consisting of ITO/c-TiO2/perovskite/Spiro-OMeTAD/Ag. The cross-sectional SEM image of the PSC is given in Figure S4. For Cs/DMA, we varied the Cs to DMA ratio (Table S1) and found the optimum power conversion efficiency (PCE) was achieved using 70% Cs and 30% DMA (Figure S5), corresponding to a bandgap of 1.70 eV. The $J-V$ curve of the champion device is given in Figure 4a. The champion device

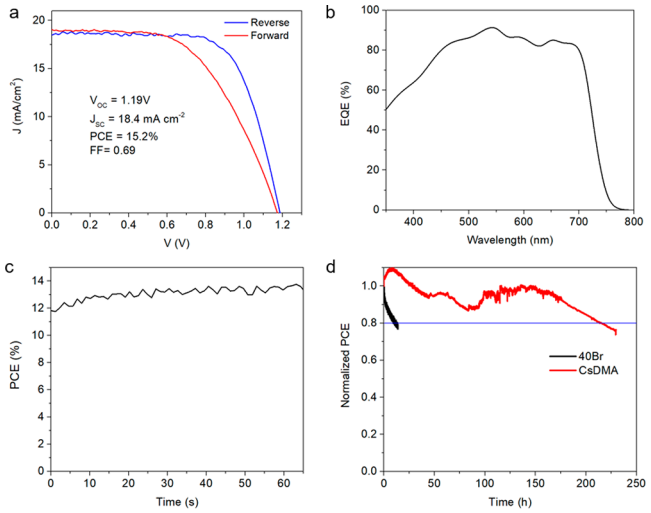

Figure 4. CsDMA device characterization. (a) $J-V$ characteristics of the champion device under simulated AM 1.5G solar illumination of 100 mW cm^{-2}. (b) EQE spectrum of the champion device. (c) Stable output at MPP, the champion device stabilizes at 13.5%. (d) Stability of an unencapsulated device under continuous white light LED illumination (100 mW cm^{-2}) at MPP in N2.

has a V_{OC} of 1.19 V, a J_{SC} of 18.4 mA cm^{-2}, and PCE of 15.2%. We achieved a V_{OC} higher than that reported in pure $CsPbI_3$ PSCs; it is 80 meV higher than in champion reports of $CsPbI_3$.[14] Figure 4b gives the external quantum efficiency of the champion device, and it corresponds to an integrated photocurrent of 18.2 mA cm^{-2}. The stabilized output at the maximum power point (MPP) is 13.5% (Figure 4c). For CsGua, a similar optimization was carried out, but a maximum PCE of only 3.65% was achieved, possibly due to the impure phase of $GuaPbI_3$ and Gua_2PbI_4 (Figure S6).

We, then, checked the operational stability of the CsDMA perovskite PSCs. Since conventional wide-bandgap perovskites with Br content 30−40% are unstable due to the Hoke effect,[17] we also fabricated PSCs using 40% Br perovskite active layers (Figure S7) using the same n-i-p structure to compare with the CsDMA devices herein.[18] The 40% Br perovskite devices degrade rapidly to below 80% of initial PCE when operated at MPP operation for 12 h, while CsDMA devices are stable for 230 h under same conditions (Fig. 4d).

In summary, the present work reports stable, wide-bandgap, bromine-free perovskites. In contrast with CsMAFAPbIBr perovskite, we were able to tune the crystal lattice by incorporating even larger cations at a lower concentration. We demonstrate that by mixing $CsPbI_3$ with another A-site cation with an ionic radius between 272 and 278 pm—DMA or Gua—it is possible to form tetragonal perovskites that are stable at room temperature. Here, the large DMA or Gua cations are incorporated in the final lattice instead of being used as an additive. The mixed perovskite yields 14-60 times longer PL lifetimes than pure $CsPbI_3$, suggesting a lower trap state density. We achieved a PCE of 15.2% and a V_{oc} of 1.19 V. The V_{oc} of the CsDMA devices is higher than in prior reports of pure CsPbI3 PSCs. The devices operated stably over 230 h at MPP, which is nearly 20 times longer than for the case of 40% Br wide-bandgap perovskites. This study extends the materials selection range for stable wide-bandgap perovskites.

https://dx.doi.org/10.1021/acsmaterialslett.0c00166
ACS Materials Lett. 2020, 2, 869−872

■ ASSOCIATED CONTENT

Supporting Information

The Supporting Information is available free of charge at https://pubs.acs.org/doi/10.1021/acsmaterialslett.0c00166.

Experimental details, XPS of N signal in $Cs_{0.7}DMA_{0.3}$ perovskite, XRD of pure $CsPbI_3$ film after aging in air for 30 min, TGA of $Cs_{0.7}DMA_{0.3}PbI_3$, cross-sectional SEM image of CsDMA perovskite, performance of different CsDMA solar cells, and $J-V$ plots of CsDMA solar cell with different DMA concentration, CsGua solar cell, and CsMAFA solar cell with 40% Br (PDF)

■ AUTHOR INFORMATION

Corresponding Author

Edward H. Sargent − *Department of Electrical and Computer Engineering, University of Toronto, Toronto, Ontario M5S 1A4, Canada;* orcid.org/0000-0003-0396-6495; Email: ted.sargent@utoronto.ca

Authors

Ziru Huang − *Department of Electrical and Computer Engineering, University of Toronto, Toronto, Ontario M5S 1A4, Canada;* orcid.org/0000-0001-7983-913X

Bin Chen − *Department of Electrical and Computer Engineering, University of Toronto, Toronto, Ontario M5S 1A4, Canada*

Laxmi Kishore Sagar − *Department of Electrical and Computer Engineering, University of Toronto, Toronto, Ontario M5S 1A4, Canada;* orcid.org/0000-0002-7656-7308

Yi Hou − *Department of Electrical and Computer Engineering, University of Toronto, Toronto, Ontario M5S 1A4, Canada;* orcid.org/0000-0002-1532-816X

Andrew Proppe − *Department of Electrical and Computer Engineering and Department of Chemistry, University of Toronto, Toronto, Ontario M5S 1A4, Canada;* orcid.org/0000-0003-3860-9949

Hao-Ting Kung − *Department of Materials Science and Engineering, University of Toronto, Toronto, Ontario M5S 3E4, Canada*

Fanglong Yuan − *Department of Electrical and Computer Engineering and Department of Materials Science and Engineering, University of Toronto, Toronto, Ontario M5S 1A4, Canada*

Andrew Johnston − *Department of Electrical and Computer Engineering, University of Toronto, Toronto, Ontario M5S 1A4, Canada;* orcid.org/0000-0002-4545-532X

Makhsud I. Saidaminov − *Department of Electrical and Computer Engineering, University of Toronto, Toronto, Ontario M5S 1A4, Canada; Department of Chemistry and Electrical and Computer Engineering, Centre for Advanced Materials and Related Technologies (CAMTEC), University of Victoria, Victoria V8P 5C2, Canada;* orcid.org/0000-0002-3850-666X

Eui Hyuk Jung − *Department of Electrical and Computer Engineering, University of Toronto, Toronto, Ontario M5S 1A4, Canada;* orcid.org/0000-0002-2833-522X

Zheng-Hong Lu − *Department of Materials Science and Engineering, University of Toronto, Toronto, Ontario M5S 3E4, Canada;* orcid.org/0000-0003-2050-0822

Shana O. Kelley − *Department of Chemistry and Department of Pharmaceutical Sciences, Leslie Dan Faculty of Pharmacy, University of Toronto, Toronto, Ontario M5S 3G4, Canada;* orcid.org/0000-0003-3360-5359

Complete contact information is available at: https://pubs.acs.org/10.1021/acsmaterialslett.0c00166

Notes

The authors declare no competing financial interest.

■ ACKNOWLEDGMENTS

This work was supported by Ontario Research Fund-Research Excellence program (ORF7-Ministry of Research and Innovation, Ontario Research Fund-Research Excellence Round 7) and US Department of the Navy, Office of Naval Research (Grant Award No. N00014-17-1-2524).

■ REFERENCES

(1) Green, M. A.; et al. The emergence of perovskite solar cells. *Nat. Photonics* **2014**, *8*, 506−514.

(2) Leijtens, T.; et al. Opportunities and challenges for tandem solar cells using metal halide perovskite semiconductors. *Nat. Energy* **2018**, *3*, 828−838.

(3) Stoddard, R. J.; et al. Enhancing Defect Tolerance and Phase Stability of High-Bandgap Perovskites via Guanidinium Alloying. *ACS Energy Lett.* **2018**, *3*, 1261−1268.

(4) Lin, R.; et al. Monolithic all-perovskite tandem solar cells with 24.8% efficiency exploiting comproportionation to suppress Sn(ii) oxidation in precursor ink. *Nat. Energy* **2019**, *4*, 864.

(5) Gharibzadeh, S.; et al. Record Open-Circuit Voltage Wide-Bandgap Perovskite Solar Cells Utilizing 2D/3D Perovskite Heterostructure. *Adv. Energy Mater.* **2019**, *9*, 1803699.

(6) Bush, K.A.; et al. Compositional Engineering for Efficient Wide Band Gap Perovskites with Improved Stability to Photoinduced Phase Segregation. *ACS Energy Lett.* **2018**, *3*, 428−435.

(7) Eperon, G. E.; et al. Inorganic caesium lead iodide perovskite solar cells. *J. Mater. Chem. A* **2015**, *3*, 19688.

(8) Chen, S.; et al. Exploring the stability of novel wide bandgap perovskites by a robot based high throughput approach. *Adv. Energy Mater.* **2018**, *8*, 1701543.

(9) Ke, W.; et al. Myths and reality of HPbI 3 in halide perovskite solar cells. *Nat. Commun.* **2018**, *9*, 4785.

(10) Li, Z.; et al. Stabilizing Perovskite Structures by Tuning Tolerance Factor: Formation of Formamidinium and Cesium Lead Iodide Solid-State Alloys. *Chem. Mater.* **2016**, *28*, 284−292.

(11) Zhao, B.; et al. Thermodynamically Stable Orthorhombic γ-CsPbI3 Thin Films for High-Performance Photovoltaics. *J. Am. Chem. Soc.* **2018**, *140*, 11716−11725.

(12) Sun, J.-K.; et al. Polar Solvent Induced Lattice Distortion of Cubic CsPbI3 Nanocubes and Hierarchical Self-Assembly into Orthorhombic Single-Crystalline Nanowires. *J. Am. Chem. Soc.* **2018**, *140*, 11705−11715.

(13) Fan, Z.; et al. Layer-by-Layer Degradation of Methylammonium Lead Tri-iodide Perovskite Microplates. *Joule* **2017**, *1*, 548−562.

(14) Wang, Y.; et al. Thermodynamically stabilized β-CsPbI3-based perovskite solar cells with efficiencies >18%. *Science* **2019**, *365*, 591−595.

(15) Wang, P.; et al. Solvent-controlled growth of inorganic perovskite films in dry environment for efficient and stable solar cells. *Nat. Commun.* **2018**, *9*, 2225.

(16) Kim, J.; et al. Amide-Catalyzed Phase-Selective Crystallization Reduces Defect Density in Wide-Bandgap Perovskites. *Adv. Mater.* **2018**, *30*, 1706275.

(17) Hoke, E. T.; et al. Reversible photo-induced trap formation in mixed halide hybrid perovskites for photovoltaics. *Chem. Sci.* **2015**, *6*, 613.

(18) Tan, H.; et al. Dipolar cations confer defect tolerance in wide-bandgap metal halide perovskites. *Nat. Commun.* **2018**, *9*, 3100.